ELSEVIER

Materials Science and Engineering A 437 (2006) 274–280

MATERIALS SCIENCE & ENGINEERING A

www.elsevier.com/locate/msea

Improvement of mechanical properties of aluminum die casting alloy by multi-pass friction stir processing

K. Nakata [a,*], Y.G. Kim [a], H. Fujii [a], T. Tsumura [a], T. Komazaki [b]

[a] *Joining and Welding Research Institute, Osaka University, 11-1 Mihogaoka, Ibaraki, Osaka 567-0047, Japan*
[b] *Ryobi Limited, 5-2-8 Toshima, Kita-ku, Tokyo 114-8518, Japan*

Received 9 May 2006; received in revised form 14 July 2006; accepted 28 July 2006

Abstract

An improvement in the mechanical properties was accomplished due to the microstructural modification of an aluminum die casting alloy by multi-pass friction stir processing (MP-FSP), which is a solid-state microstructural modification technique using a frictional heat and stirring action. The hardness of the MP-FSP sample is about 20 Hv higher than that of the base metal. The tensile strengths of the MP-FSPed specimens were significantly increased to about 1.7 times versus that of the base metal. This is due not only to the disappearance of the cold flake in the base metal, but also to a structural refinement, such as uniform distribution of Si particles. Thus, the application of the MP-FSP is a very effective method for the mechanical improvement of aluminum die casting alloys.

Keywords: Friction stir processing; Mechanical properties; Hardness; Tensile strength; Cold flake

1. Introduction

Friction stir processing (FSP), which is a solid-state microstructural modification technique using a friction heat and stirring action, has recently attracted attention for making aluminum alloys with an excellent specific strength, and its studies have been actively performed [1–12]. This process is the outgrowth of the basic principle of friction stir welding (FSW) [13], and the mechanical properties of the FSPed material are improved due to the grain refinement of the microstructural modification [2,3,5,6,7,9].

Aluminum die casting alloys are made by the rapid injection of molten metal into metal molds under high pressure. These alloys have a dense and fine grain surface, and are easily made by mass production. However, a casting defect and an abnormal structure, such as a cold flake, are easily formed in the base metal; these are caused by the destruction of the solidified layers in a metal sleeve [14–17]. These defects significantly degrade the mechanical properties of the base metal.

From this point of view, the FSP should be effective for the improvement of mechanical properties of the aluminum die casting alloys. However, the FSP of die casting alloys has not previously been reported.

In this study, the multi-pass FSP (MP-FSP) technique [18,19] was performed using an ADC12 aluminum die casting alloy to obtain a wide-area improvement, and the mechanical properties of the MP-FSP samples were evaluated. Particularly, the effects of the cold flake, which is a distinctive defect of the die cast alloys, and the structural refinement on the tensile strength were individually investigated.

2. Experimental procedures

Four-millimeter thick plates of ADC12 aluminum die casting alloys were used in this study. Table 1 lists the chemical composition of the base metal.

In order to estimate the effect of the MP-FSP on the structure modification of the ADC12 alloy, the stir-in-plate FSP was performed using a load control type FSW machine. The FSW tool has a columnar shape with a screw probe. The diameter of the tool shoulder is 15 mm. The diameter of the tool probe is 5 mm and its length is 3.9 mm. SKD61 was used as the tool material. The tilt angle is 3°. Mild steel was used for the backing plate. FSP was continuously performed 14 times by moving in 4 mm increments toward the advancing side.

* Corresponding author. Tel.: +81 6 6879 8656; fax: +81 6 6879 8689.
E-mail address: nakata@jwri.osaka-u.ac.jp (K. Nakata).

0921-5093/$ – see front matter © 2006 Elsevier B.V. All rights reserved.
doi:10.1016/j.msea.2006.07.150

Table 1
Chemical compositions of ADC12 base material

Alloy	Chemical compositions (mass%)									
	Cu	Si	Mg	Zn	Fe	Mn	Ni	Sn	Pb	Al
ADC12	2.35	11.82	0.17	0.56	0.81	0.18	0.04	0.02	0.06	Bal.

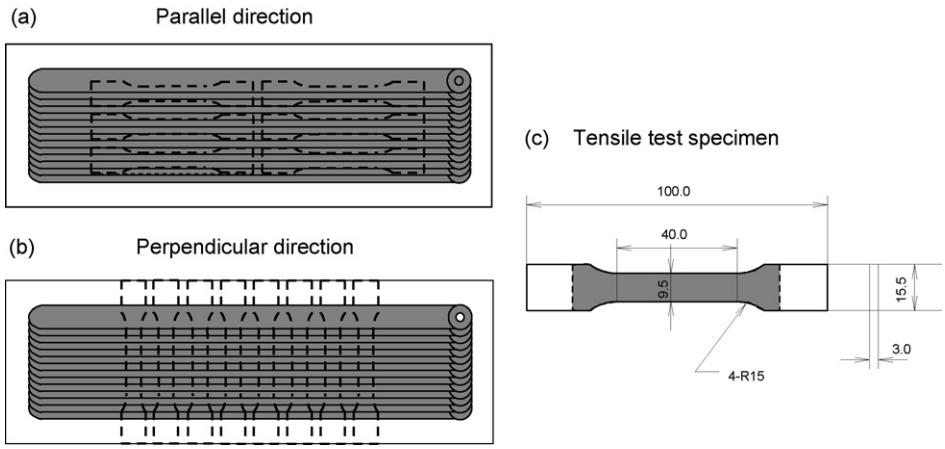

Fig. 1. Cutting direction and dimension of the tensile test specimens of MP-FSP samples.

As for the processing parameters, the tool plunge downforce was 14.2 kN, the tool rotation speed was 1250 min^{-1} and the plate travel speed was 500 mm/min [20,21].

After the FSP, a metallurgical inspection was performed on cross-sections of the sample. They were polished and etched with a 5% hydrofluoboric acid (HBF_4) water solution for the optical microscopic (OM) observations. The Vickers hardness of a transverse cross-section of the MP-FSP sample was measured using a hardness testing machine (Akashi, AAV-500) with 0.98 N loads. The tensile test was performed for both the base metal and the MP-FSPed specimens. The tensile test specimens were cut parallel and perpendicular to the MP-FSP direction. The specimen dimensions are shown in Fig. 1.

The aluminum matrix structure in the stir zone (SZ) was observed by TEM. For the TEM, a thin disk specimen of 120 μm and 3 mm in diameter, was cut from the middle part of the SZ and was prepared by twin-jet electropolishing in a 30% nitric acid/methanol solution. The TEM observation was carried out using a Hitachi H-800 transmission electron microscope operating at 200 KV.

3. Results and discussion

3.1. Quality of MP-FSP samples

Fig. 2 shows the bead appearance and X-ray radiography of the MP-FSP sample. It is clearly seen that a smooth surface was obtained and no inner defect, such as a cavity, was observed

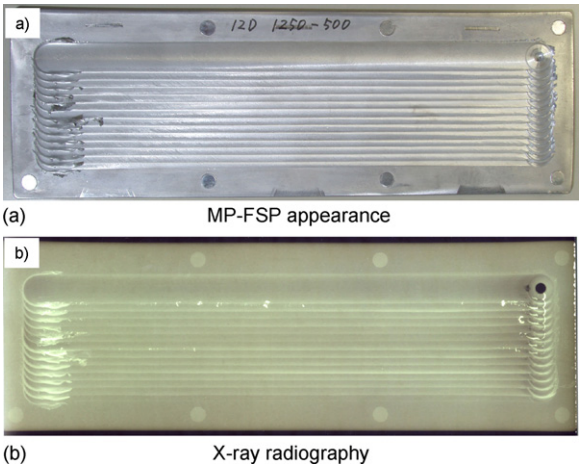

Fig. 2. Surface appearance and X-ray radiography of the MP-FSP sample.

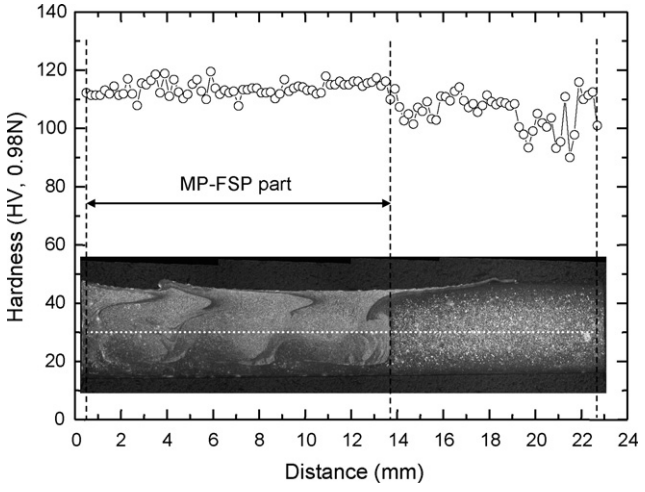

Fig. 3. Hardness profile of cross-section in the MP-FSP sample.

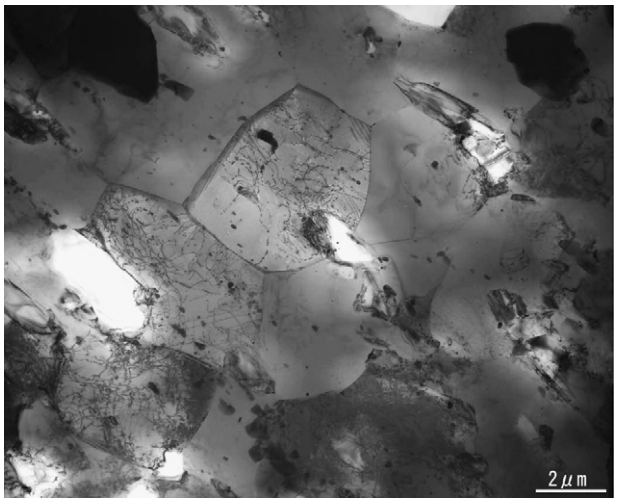

Fig. 4. TEM image of the middle part in stir zone of ADC12 FSW joints. (14.2 kN, 1250 min^{-1}, 500 mm/min).

analysis for a wide area (57 mm (w) × 260 mm (l)) inside the sample based on the X-ray radiography.

3.2. Hardness of MP-FSP samples

Fig. 3 shows the hardness profile of a cross-section of the MP-FSP sample. In the macroscopic structure, the MP-FSPed part is sound without any defects. The modification zone is widely and continuously observed. The hardness of the MP-FSP part is a uniform 110 Hv, which is about 20 Hv higher than that of the base metal. The hardness of the base metal is quite variable. It is considered that the hardness increase in the MP-FSPed part is due to deleting the casting defect, a fine dispersion of Si particles and the grain refinement [9,21]. Santella et al. [9] reported the microstructural and mechanical properties of the FSP of two Al castings, A356 and A319. For the microstructural features, the stirring action reduced the porosity, fractured large second-phase particles reducing both their average size and aspect ratios. Fujii et al. [21] also discussed the effect of the welding parameters on the size, the aspect ratio and the direction angle of the Si particles for each FSW condition. During the FSW, the Si particles should be easy to break down due to the plastic flow, and the finer Si particles were uniformly formed in the SZ.

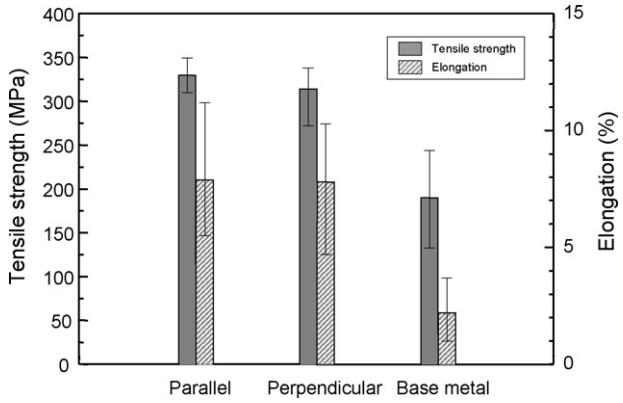

Fig. 5. Tensile test results of base metal and MP-FSP samples for different directions.

Moreover, the grain refinement significantly should contribute to the hardness increase. Fig. 4 shows a TEM image of the middle part in the SZ. The grain size of the Al matrix in the ADC12 base metal was roughly 7–20 μm, however, the grain

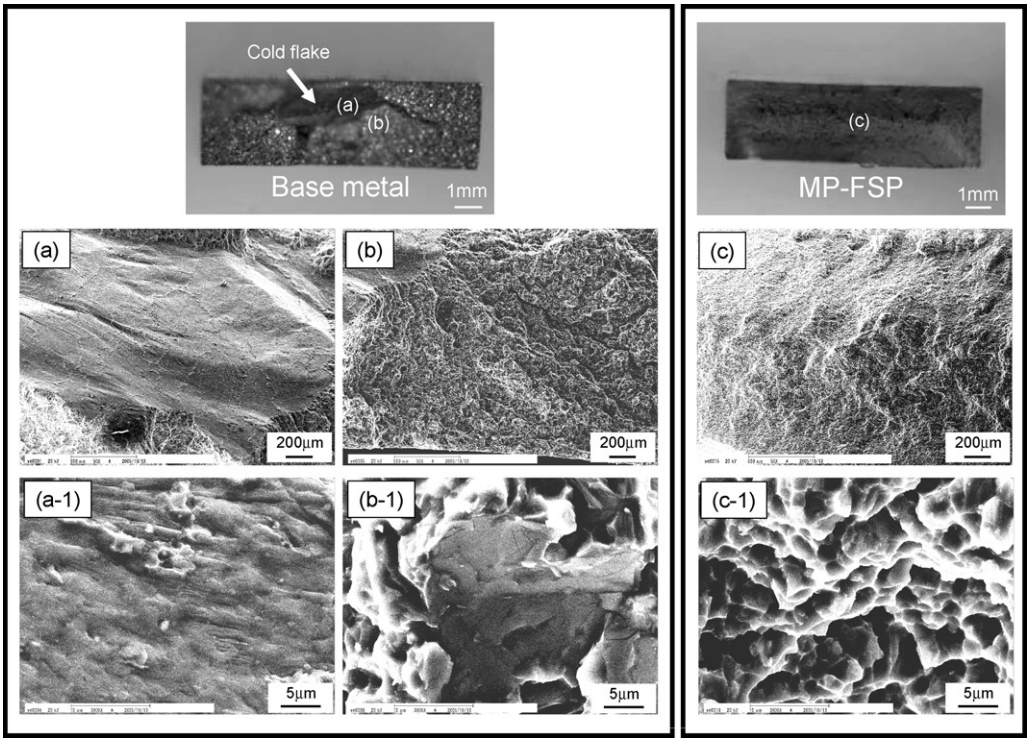

Fig. 6. Fracture surface of tensile test specimens in the base metal and the MP-FSP sample; (a-1), (b-1) and (c-1) high magnification of (a), (b) and (c).

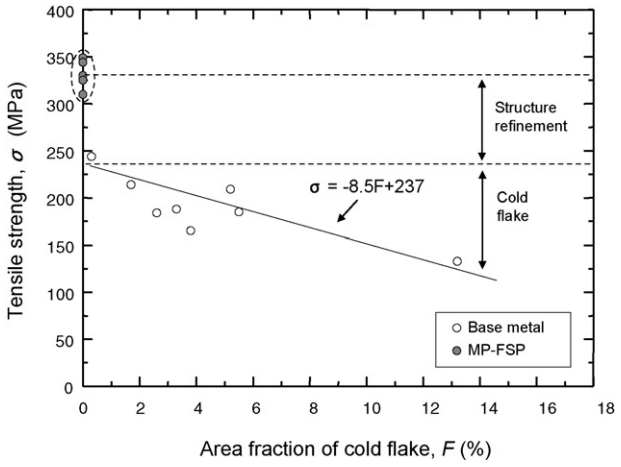

Fig. 7. Relationship between area fraction of cold flake at the fracture surface and tensile strength of ADC12 base metal and MP-FSP samples.

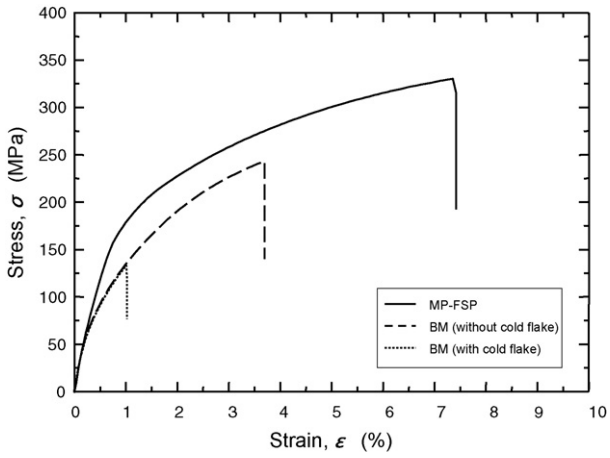

Fig. 8. Comparison of the tensile behaviors of the MP-FSP for the base metal without and with cold flake.

size of the middle part in the SZ formed a very fine structure of about 2–3 μm due to the dynamic recrystallization. Based on related past studies, the relationship between the hardness Hv in the SZ and the grain size d have been examined using the Hall–Petch equation [22].

$$\mathrm{Hv} = H_0 + k_\mathrm{H} d^{-1/2} \quad (1)$$

where H_0 and k_H are appropriate constants. Because Hv is proportional to $d^{-1/2}$, the finer the grain size is, the higher the hardness value is. For example, the extrapolated values for the boundary-free condition and slope of the Hall–Petch equation for the 1050 pure aluminum alloy welds are $H_0 = 18.2$ Hv and $k_\mathrm{H} = 18.9\ \mathrm{Hv\ mm^{-1/2}}$ [22]. From Eq. (1), the SZ with a grain size between 2 and 3 μm has an average hardness of about 31 Hv (32–29 Hv), and the base metal with a grain size between 7

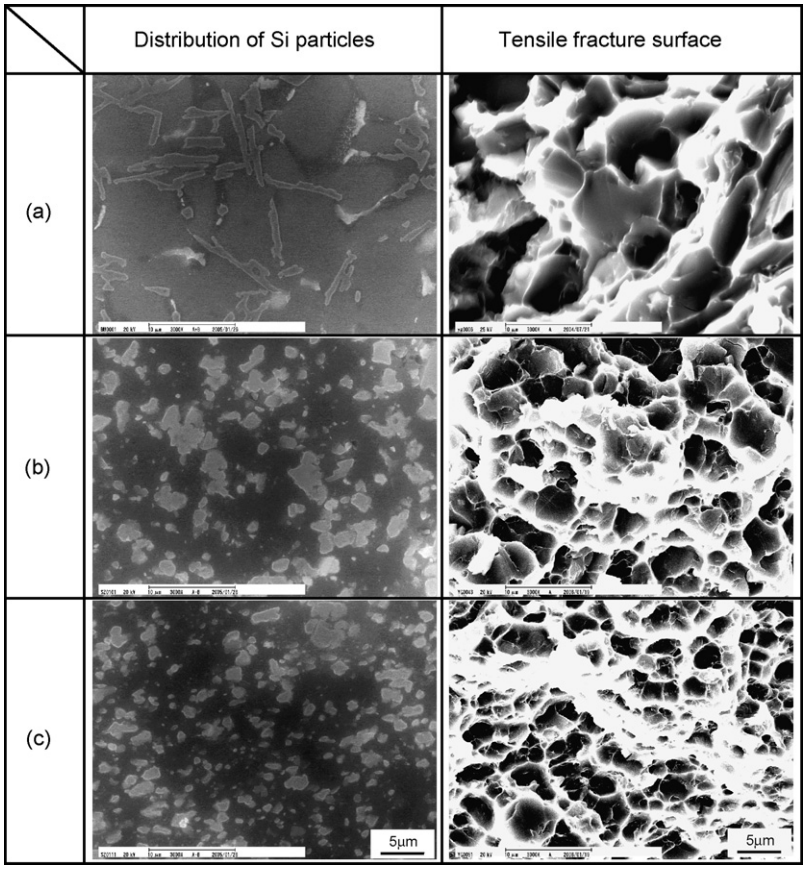

Fig. 9. Relationship between distribution of Si particles and tensile fracture surface in FSW joint: (a) base metal, (b) middle part of the stir zone and (c) bottom part of the stir zone at 14.2 kN, 1250 $\mathrm{min^{-1}}$, 500 mm/min.

and 20 μm has an average hardness of about 24 Hv (25–22 Hv). Thus, this difference is not very significant.

3.3. Tensile properties of MP-FSP samples

Fig. 5 shows the tensile properties of the ADC12 base metal and MP-FSPed specimens. The tensile strengths of the MP-FSPed specimens are much higher than that of the base metal. The average tensile strength of 330 MPa in the parallel direction increased by about 1.7 times over that of the base metal of 190 MPa, though the strength is significantly scattered in the base metal similar to the hardness profile. In any case, the elongation of the MP-FSP samples is higher than the base metal; the average of 7.8% increases by about 3.5 times over that of the base metal of 2.2%. The factors increasing the tensile strength for the MP-FSP samples can be as follows:

(1) elimination of the casting defects (such as porosity and cold flake);
(2) uniform dispersion of the finer Si particles;
(3) grain refinement of aluminum matrix.

Fig. 6 shows the appearance and SEM images for the typical fracture surface of the base metal and MP-FSP sample. A coarse fracture structure type is clearly observed in the base metal, which has cold flake as a partly brittle fracture. However, a fine ductile fracture was obtained after the MP-FSP and the cold flake was hardly seen. Based on this result, it is clear that the cold flake should significantly affect the tensile properties.

In order to analyze the effect of the cold flake, the relationship between the area fraction of the cold flake and the tensile strength of the ADC12 base metal and MP-FSPed specimens in the parallel direction was investigated, as shown in Fig. 7. The fraction of the cold flake was determined for each fracture surface. The tensile strengths of the MP-FSPed specimens are much higher than that of the base metal. It is noted that for the base metal, the tensile strength can be classified by the area fraction of the cold flake. It increases with the decreasing area fraction of the cold flake. Considering the relationship between the tensile strength of the base metal and the area fraction of the cold flake, the following equation is obtained.

$$\sigma = -8.5F + 237 \quad (2)$$

where σ is the tensile strength of the base metal (MPa), and F is the area fraction of the cold flake (%). In the MP-FSPed specimens, on the other hand, the cold flake completely disappears and the tensile strength is much higher than that of the base metal even when no cold flake exists (237 MPa). Thus, it is clear that the tensile strength increases are due not only to the disappearance of the cold flake, but also to the structural refinement in the die cast alloy.

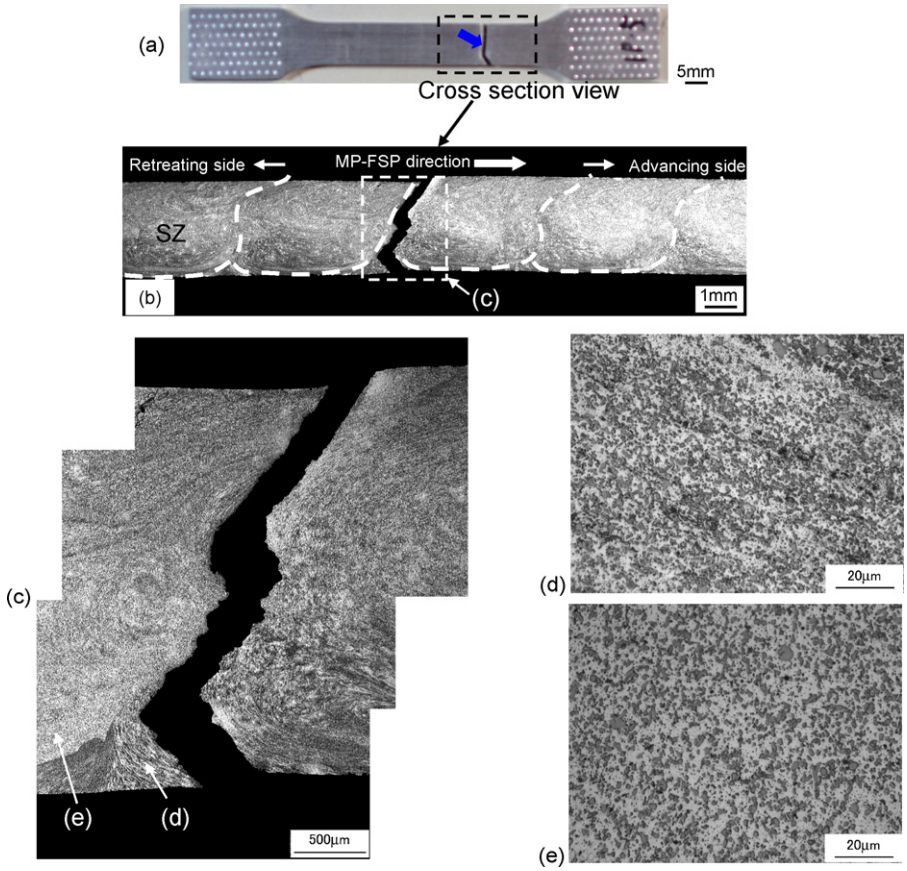

Fig. 10. Tensile failure view of: (a) tensile test specimen of a perpendicular direction for MP-FSP, (b) cross-section showing fracture position and (c), (d), (e) are magnified optical micrographs in (b).

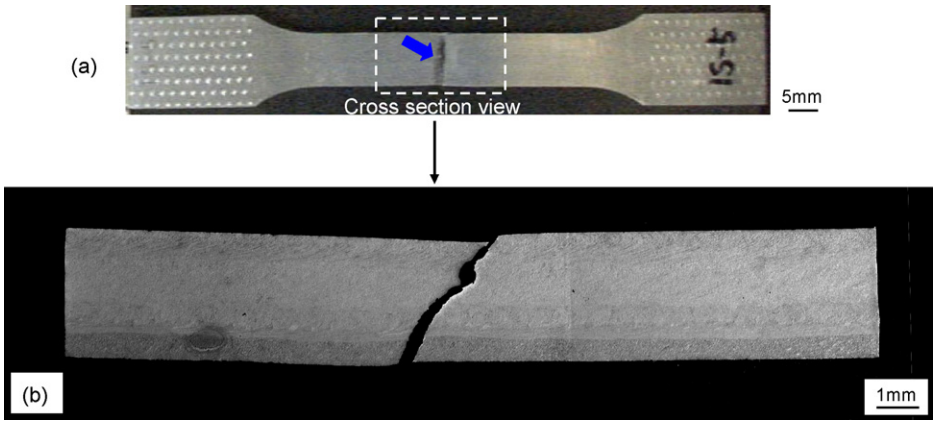

Fig. 11. Tensile failure view of: (a) tensile test specimen of a parallel direction for MP-FSP and (b) cross-section showing fracture position.

Fig. 8 shows the stress–strain diagram of the base metal and MP-FSPed sample. Each stress–strain curve of the base metal seems to be collinear, though the base metal with cold flake fractures more easily than the one without the cold flake. However, for the MP-FSP sample, the 0.2% proof stress as well as the elongation increase, because the grain refinement of the Al matrix and the fine dispersion of the Si particles occur.

Based on the tensile fracture, it is easily found that the effect of the distribution of the Si particles was significant, as shown in Fig. 9. Typically, the base metal has long-bar shaped Si particles and large dimples. On the other hand, the SZ has a different Si particle distribution in the other regions, i.e., the number of finer Si particles increases in the bottom part compared to the middle part [21]. Also, the dimples in the bottom are smaller than those in the middle part. Thus, the distribution of the Si particles was almost the same for the dimples in the base metal and FSW joint in each tensile fracture surface. Accordingly, it is postulated that the effect of the dispersion of the finer Si particles is larger compared to the grain refinement on the increasing tensile strength.

3.4. Effect of welding direction

Comparing the tensile results of the two tensile test directions for the MP-FSP samples, the tensile strength was not significantly scattered in the case of the parallel direction; the average strength of 330 MPa was higher than that of 314 MPa in the perpendicular direction, as shown in Fig. 5. As shown in Figs. 10 and 11, the reason for the different strengths is theorized to be due to the tensile failure structure. The failure position was along the thermo-mechanically affected zone (TMAZ) in the perpendicular direction, although in the case of the parallel direction, the tensile failure occurred in the SZ. Near the fracture position in the perpendicular direction, Fig. 10(d) clearly shows plastic deformation structures and the finer Si particles are significantly aligned in a particular direction. This degrades the tensile strength of the TMAZ. Therefore, in the perpendicular direction, the TMAZ was a weak spot for tensile fracture, as shown in Fig. 10.

4. Conclusions

The following conclusions were derived from the results of this study.

(1) The tensile strengths of the MP-FSPed specimens are much higher than that of the base metal. The average tensile strength in the parallel direction is 330 MPa, which is higher than 314 MPa in the perpendicular direction. The elongations of the two MP-FSP directions were almost the same.
(2) The tensile strength increases with the decreasing area fraction of the cold flake in the base metal. The tensile strength of the base metal without any cold flake is estimated to be 237 MPa.
(3) The main factors increasing the tensile strength for the MP-FSP samples are considered as (1) elimination of the cold flakes and (2) uniform dispersion of the finer Si particles.

Acknowledgments

This work was supported by a Grant-in-Aid for the Cooperative Research Project of Nationwide Joint-Use Research Institutes on Development Base of Joining Technology for New Metallic Glasses and Inorganic Materials from the Ministry of Education, Culture, Sports, Science and Technology of Japan, and a Grant-in-Aid for Science Research from the Japan Society for Promotion of Science.

References

[1] R.S. Mishra, M.W. Mahoney, S.X. Mcfadden, N.A. Mara, A.K. Mukherjee, Scripta Mater. 42 (2000) 163–168.
[2] P.B. Berbon, W.H. Bingel, R.S. Mishra, C.C. Bampton, M.W. Mahoney, Scripta Mater. 44 (2001) 61–66.
[3] Z.Y. Ma, R.S. Mishra, M.W. Mahoney, Acta Mater. 50 (2002) 4419–4430.
[4] R.S. Mishra, Z.Y. Ma, I. Charit, Mater. Sci. Eng. A 341 (2003) 307–310.
[5] Y.J. Kwon, I. Shigematsu, N. Saito, J. Jpn. Inst. Met. 67 (2003) 547–554.
[6] H.J. Liu, H. Fujii, K. Nogi, Mater. Sci. Tech. 20 (2004) 399–402.
[7] Z.Y. Ma, R.S. Mishra, M.W. Mahoney, Scripta Mater. 50 (2004) 931–935.
[8] S.R. Sharma, Z.Y. Ma, R.S. Mishra, Scripta Mater. 51 (2004) 237–241.
[9] M.L. Santella, T. Engstrom, D. Storjohann, T.Y. Pan, Scripta Mater. 53 (2005) 201–206.

[10] I. Charit, R.S. Mishra, Acta Mater. 53 (2005) 4211–4223.
[11] R.S. Mishra, Z.Y. Ma, Mater. Sci. Eng. R 50 (2005) 1–78.
[12] J.Q. Su, T.W. Nelson, C.J. Sterling, Mater. Sci. Eng. A 405 (2005) 277–286.
[13] W.M. Thomas, International Patent Application No. PCT/GB92/02203 and GB Patent Application No. 9125978.8, 6, U.S. Patent No. 5,460,317, 1991.
[14] H. Iwahori, K. Tozawa, Y. Yamamoto, M. Nakamura, J. Jpn. Inst. Light Met. 34 (1984) 389–394.
[15] H. Iwahori, K. Tozawa, T. Asano, Y. Yamamoto, M. Nakamura, S. Uenishi, J. Jpn. Inst. Light Met. 34 (1984) 525–530.
[16] T. Komazaki, Y. Maruyama, N. Nishi, Imono (J. Jpn. Foundarymen's Soc.) 67 (1995) 258–264.
[17] K. Kanazawa, M. Okayasu, Trans. Jpn. Soc. Mech. Eng. 64 (1998) 1878–1963.
[18] J.Q. Su, T.W. Nelson, C.J. Sterling, Scripta Mater. 52 (2005) 135–140.
[19] Y.S. Sato, S.H.C. Park, A. Matsunaga, A. Honda, H. Kokawa, Mater. Sci. 40 (2005) 637–642.
[20] Y.G. Kim, H. Fujii, T. Tsumura, T. Komazaki, K. Nakata, Mater. Sci. Eng. A 415 (2006) 250–254.
[21] H. Fujii, Y.G. Kim, T. Tsumura, T. Komazaki, K. Nakata, Mater. Trans. 47 (2006) 224–232.
[22] Y.S. Sato, S.H.C. Park, H. Kokawa, Metall. Mater. Trans. 32A (2001) 3033–3042.